Assessment of the thermoelectric performance of polycrystalline p-type SnSe

Selma Sassi, Christophe Candolfi, Jean-Baptiste Vaney, Viktoriia Ohorodniichuk, Philippe Masschelein, Anne Dauscher, Bertrand Lenoir

Assessment of the thermoelectric performance of polycrystalline p-type SnSe

S. Sassi, C. Candolfi, J.-B. Vaney, V. Ohorodniichuk, P. Masschelein, A. Dauscher, and B. Lenoir

Citation: Applied Physics Letters **104**, 212105 (2014); doi: 10.1063/1.4880817
View online: http://dx.doi.org/10.1063/1.4880817
View Table of Contents: http://scitation.aip.org/content/aip/journal/apl/104/21?ver=pdfcov
Published by the AIP Publishing

Assessment of the thermoelectric performance of polycrystalline *p*-type SnSe

S. Sassi, C. Candolfi, J.-B. Vaney, V. Ohorodniichuk, P. Masschelein, A. Dauscher, and B. Lenoir[a)]
Institut Jean Lamour, UMR 7198 CNRS—Université de Lorraine, Parc de Saurupt, CS 50840, 54011 Nancy, France

(Received 2 May 2014; accepted 18 May 2014; published online 30 May 2014)

We report the evaluation of the thermoelectric performance of polycrystalline *p*-type SnSe, a material in which unprecedented values of the thermoelectric figure of merit *ZT* have been recently discovered in single crystals. Besides anisotropic transport properties, our results confirm that this compound exhibits intrinsically very low thermal conductivity values. The electrical properties show trends typical of lightly doped, intrinsic semiconductors with thermopower values reaching 500 $\mu V K^{-1}$ in a broad temperature range. An orthorhombic-to-orthorhombic transition sets in at 823 K, a temperature at which the power factor reaches its maximum value. A maximum *ZT* of 0.5 was obtained at 823 K, suggesting that proper optimization of the transport properties of SnSe might lead to higher *ZT* values. These findings indicate that this system represents an interesting experimental platform for the search of highly efficient thermoelectric materials. © *2014 AIP Publishing LLC*. [http://dx.doi.org/10.1063/1.4880817]

Thermoelectric generators provide a green and reliable source of energy that enable converting waste heat into useful electricity.[1–3] So far, thermoelectricity remains a niche technology applied in areas where the efficiency criterion is overcome by the need of reliability. A more widespread use of thermoelectric generators would be possible if their efficiency can be further improved. The dimensionless thermoelectric figure of merit *ZT* ($ZT = \alpha^2 T/\rho\kappa$) is the key material's parameter that governs the efficiency of energy conversion.[1] The design of good thermoelectric materials rests upon the ability to reach a subtle balance between electronic and thermal properties: high thermopower (α), low electrical resistivity (ρ), and low thermal conductivity (κ). These three transport coefficients are interdependent through the carrier concentration. The challenge to face is therefore to find materials that show electronic properties typical of heavily doped semiconductors combined with a poor ability to conduct heat.[4] One possible strategy to fulfill these requirements is to search for materials that possess inherently extremely low thermal conductivity values. Several families of compounds, such as among others Zintl phases, Mo-based cluster compounds, or sulphur-based compounds, have been discovered to exhibit this property, all leading to interesting *ZT* values at high temperatures.[5–10]

Very recently, an investigation of the thermoelectric performance of single-crystalline tin selenide (SnSe) has revealed that this binary alloy is another example of such compounds.[11] This material crystallizes with a layered crystal structure described within the orthorhombic *Pnma* space group. Around 800 K, it undergoes an orthorhombic-to-orthorhombic distortion, which was confirmed by high-resolution images collected with a transmission electron microscope in the selected area diffraction mode below and above the transition temperature. The high-temperature phase then possesses a unit cell described in the *Cmcm* space group. The anisotropy of the crystal structure is usually reflected in the thermal and electronic transport properties. SnSe is no exception, the electronic and thermal properties displaying significant difference in the three crystallographic directions. Though SnSe is a well-known semiconductor studied for its potential in solar cells or in phase-change memory alloys,[12,13] its thermoelectric properties have been only scarcely investigated.[14] Of particular relevance are the extremely high *ZT* values reported by Zhao *et al.*[11] that reach 2.6 and 2.3 at 950 K (i.e., in the high-temperature phase) along the *b* and *c* axes, respectively. A more moderate value (0.9 at 950 K), though still high, was reached along the *a* axis. These outstanding and record values observed along the *b* and *c* directions arise due to a favorable combination of high thermopower and extremely low thermal conductivity values presumably due to a strong anharmonicity of the chemical bonding.[11]

Yet, the use of layered single crystals in thermoelectric devices is usually prevented by their poorer mechanical properties with respect to polycrystals and by the carefully controlled conditions required to grow them. In addition, the techniques used for crystal growth makes difficult an industrial scale-up. Bismuth telluride alloys give a prominent example of these difficulties. It appears therefore essential to determine the thermoelectric potential of polycrystalline samples. Moreover, the fact that an estimation of *ZT* of an ideal polycrystal based on the results of Zhao *et al.*[11] leads to a value of ~1.9 at 800 K raises the question whether such value can be achieved in this phase. Here, we report a study of the thermoelectric properties of polycrystalline bulk SnSe between 300 and 850 K.

Polycrystalline samples of SnSe were synthesized by direct reaction of stoichiometric amounts of Sn shots (99.999%) and Se powders (99.999%) in evacuated and

a)Author to whom correspondence should be addressed. Electronic mail: bertrand.lenoir@univ-lorraine.fr

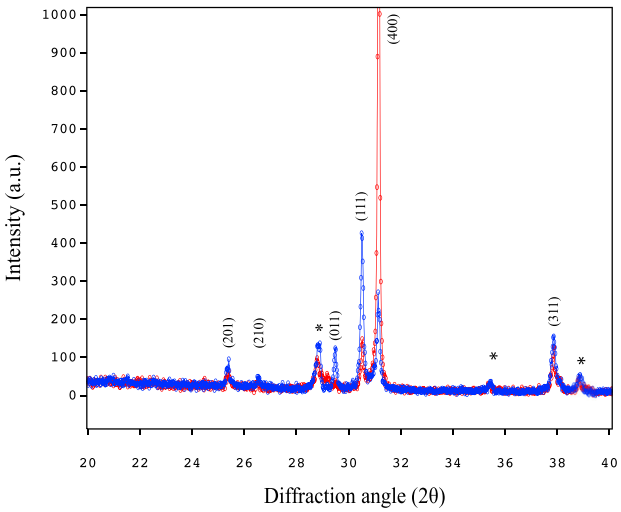

FIG. 1. Magnification of XRPD patterns around the main Bragg peaks measured on bulk samples parallel (blue color) and perpendicular (red color) to the pressing direction. The (*hkl*) values are indicated for each reflection. The asterisk corresponds to extrinsic reflections coming from the sample holder.

sealed quartz tubes. The tube, sealed under inert atmosphere, was heated up to 1223 K, dwelt at this temperature for one day, furnace-cooled to 773 K, and finally quenched in room-temperature water. The ingot was grounded in an agate mortar into fine powders that were loaded in a graphite die of 10 mm in diameter. The powders were then densified by spark plasma sintering at 698 and 708 K for 7 min under a uniaxial pressure of 50 Mpa. The crystal structure was checked by x-ray powder diffraction (XRPD) performed on a Bruker D8 Advance instrument with CuKα1 radiation at room temperature. The chemical homogeneity and composition were analyzed by combining scanning electron microscopy (SEM) and energy-dispersive x-ray spectroscopy (EDXS) analyses using a FEI Quanta FEG.

To probe the anisotropy of the transport properties, samples with well-defined dimensions (typically $2 \times 2 \times 9$ mm^3 and $6 \times 6 \times 1$ mm^3 for parallelepiped and square-shaped samples, respectively) were cut both parallel and perpendicular to the pressing direction with a diamond-wire saw. Thermopower and electrical resistivity data were collected simultaneously between 300 and 850 K using a ZEM-3 setup (Ulvac-Riko) and up to 970 K for one of the samples. Thermal conductivity was determined in the 300–850 K temperature range by combining thermal diffusivity a, specific heat C_p, and density d according to the relation $\kappa = aC_pd$. Thermal diffusivity was measured by the laser flash technique using a Netzsch LFA 427 instrument. The density was determined from the measured mass and dimensions and was considered temperature-independent. The specific heat was measured by differential scanning calorimetry using a Pegasus 403 instrument (Netzsch). The Hall coefficient was measured at 300 K by a Van der Pauw method and with the ac transport option of a physical property measurement system (PPMS). The Hall carrier concentration and Hall mobility of the charge carriers were calculated from the Hall coefficient R_H assuming a single-parabolic band model and a Hall factor of 1 according to the relations $p = 1/R_He$ and $\mu_H = R_H/\rho$, where e is the elementary charge.

The XRPD pattern collected before the sintering process could be fully indexed within the space group *Pnma* of SnSe. The lattice parameters were estimated by refining the pattern with the (h00) reflections excluded due to the strong texture of the samples. This led to $a = 11.497(3)$ Å, $b = 4.153(4)$ Å, and $c = 4.433(4)$ Å, in good agreement with literature data.[14] XRPD patterns measured before and after the sintering

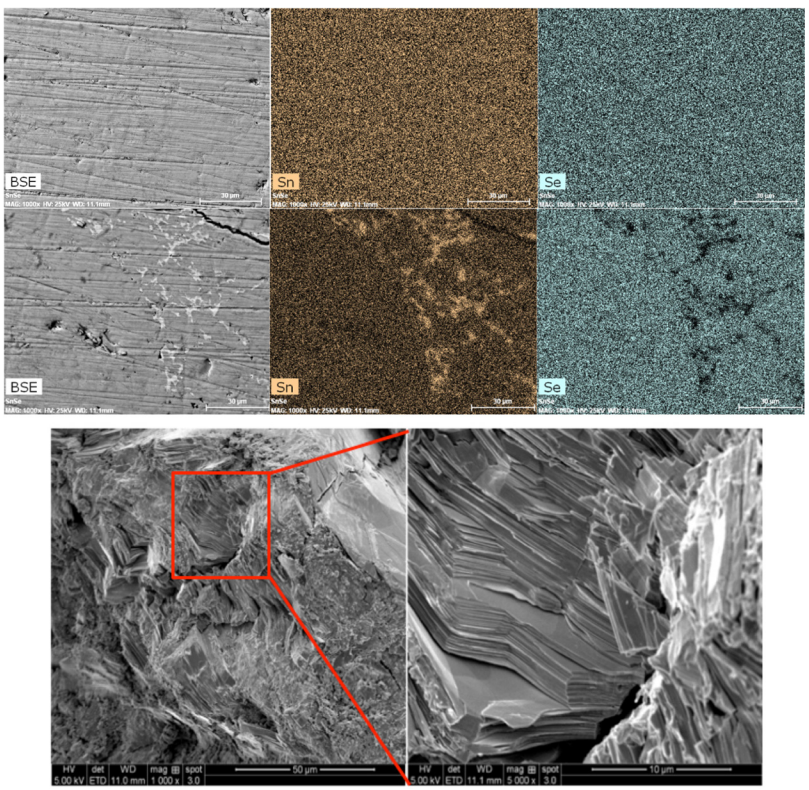

FIG. 2. (Top panels) X-ray mappings indicating a good chemical homogeneity of the samples. (Middle panels) X-ray mappings highlighting the small fraction of elemental Sn present in the samples. The scale bar stands for 30 μm in all images. (Bottom panels) SEM fracture images of SnSe after SPS treatment.

process were identical revealing no evident thermal decomposition. Analyses performed parallel and perpendicular to the pressing direction indicate marked differences in the intensity of the (400) reflection suggesting that grains have preferentially grown along these planes (Figure 1). Similar results were obtained in a prior study of Te-substituted SnSe.[14] The densities are equal to 96% and 97% of the theoretical density for the samples densified at 698 and 708 K, respectively. Though the XRPD patterns suggested the absence of secondary phases, a careful analysis of the sample by SEM revealed traces of elemental Sn (Figure 2) suggesting a slight off-stoichiometry on the Sn site. Except for rare areas where Sn is observed, X-ray mapping indicated a homogeneous distribution of Sn and Se within the sample (Figure 2). EDXS results revealed that the chemical composition of the samples is consistent with an equimolar ratio of Sn and Se.

Based on the present structural characterizations and owing to the anisotropy of the crystal structure, we may anticipate the transport properties to show some degree of anisotropy. The transport properties of each sample were therefore measured parallel and perpendicular to the pressing direction. For comparison, the data measured on single crystals by Zhao *et al.*[11] have been converted into the mean value expected in an ideal isotropic polycrystal defined as one third of the trace of the $\bar{\bar{\rho}}$, $\bar{\bar{\alpha}}$, and $\bar{\bar{\kappa}}$ tensors.

The temperature dependences of ρ and α are shown in Figures 3(a) and 3(b), respectively. ρ shows an overall decrease with increasing temperature in both directions indicative of a semiconducting behavior. A clear anomaly around 530 K is observed in the polycrystalline and, to a lesser extent, in the single crystalline samples. This anomaly does not seem to depend on the synthesis conditions and was reproduced in the two sample batches. Because the temperature at which this anomaly occurs is close to the melting point of elemental tin (505 K), the increase in ρ might be due to this effect. At 850 K, the upturn observed in the ρ data is likely related to the distortion of the unit cell. Above this temperature, ρ smoothly increases with temperature up to 900 K. This effect is probably due to the activation of minority carriers across the band gap, which appears consistent with a smaller band gap in the high-temperature phase.[11] The values of α are positive in the whole temperature range indicating that holes are the majority charge carriers. α increases from 490 μV K^{-1} at 300 K up to a maximum of approximately 510 μV K^{-1} around 500 K. The values measured in the polycrystalline samples are lower than those observed in the single crystals.[11] This difference may be due to slight variations in the hole concentrations with temperature since the value measured in the present samples is very close to that measured in single crystals ($\sim 4 \times 10^{17}$ cm^{-3} at 300 K in both directions leading to Hall mobilities of $\sim$30 and 10 cm^2 V^{-1} s^{-1} for perpendicular and parallel directions, respectively).[11] The high α values are suggestive of a lightly doped, nearly intrinsic nature of the electrical properties in SnSe. Above 500 K, α rapidly decreases due to the thermal excitation of minority carriers. Yet, unlike the results of Zhao *et al.*,[11] above the transition temperature, α does not show a nearly constant value but further decreases to reach a moderate value of 145 μV K^{-1} at 960 K. Though the origin of this discrepancy remains to be understood, the fact that α decreases seems consistent with an influence of minority carriers in this temperature range.

Noteworthy, SnSe does not appear to be stable at temperatures above the phase transition. The lack of stability is confirmed by the plastic deformation undergone by the samples at high temperatures and by the onset of thermal decomposition on their surface owing to a likely loss of Se during the measurement cycle. This is further demonstrated by a loss of mass during the measurements. Further work is required to determine the maximum temperature at which this material may safely operate. The maximum value of the power factor (α^2/ρ) was 4×10^{-4} W m^{-1} K^{-2} at 820 K. This value is lower than that measured by Zhao *et al.*[11] in the *b* and *c* directions due to higher ρ values in polycrystalline samples.

Figure 4(a) presents the temperature dependence of the total thermal conductivity κ. Because of the high ρ values, the electronic contribution to the thermal conductivity becomes sizeable only above 600 K. The measured values thus almost entirely reflect the lattice component. Very low

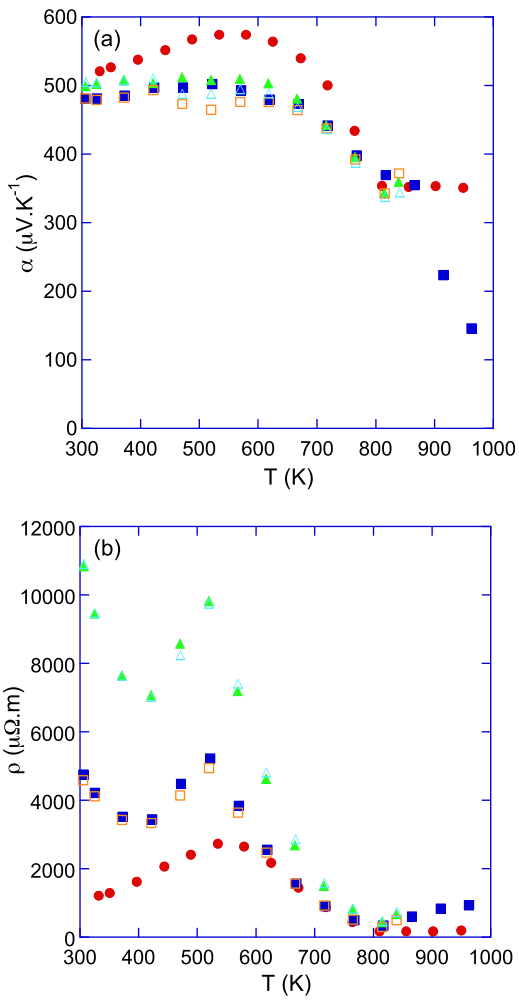

FIG. 3. Temperature dependence of the electrical properties of SnSe measured in both directions: (a) thermopower α and (b) electrical resistivity ρ. Both properties were measured parallel (triangle symbols) and perpendicular (square symbols) to the pressing direction in two different samples (sample 1 filled symbols and sample 2 open symbols). The mean value of the data collected on single crystals has been added for comparison (filled circle symbols).

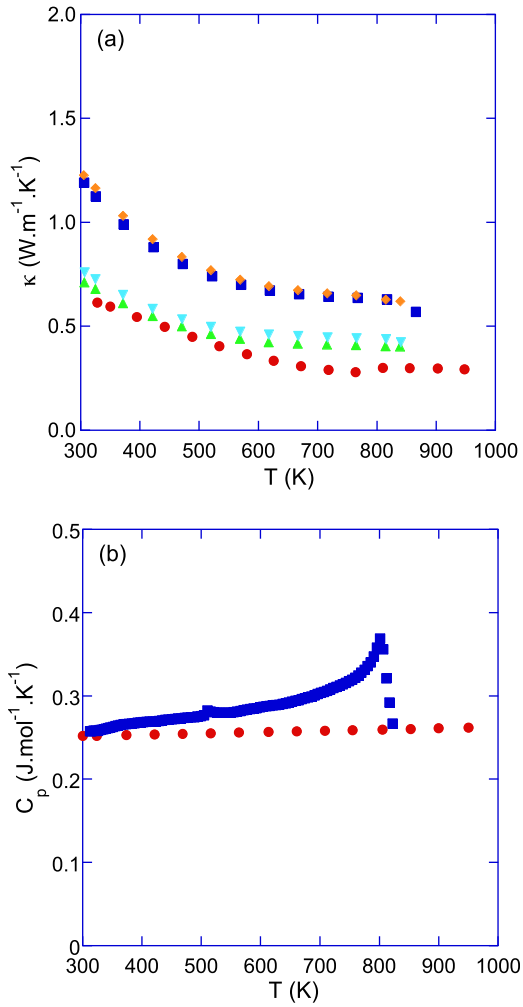

FIG. 4. (a) Temperature dependence of the total thermal conductivity κ of polycrystalline bulk samples of SnSe measured parallel and perpendicular to the pressing direction. The mean value of the data obtained on single crystals by Zhao *et al.*[11] has been added for comparison. (b) Specific heat data as a function of temperature in polycrystalline (square symbol) and single-crystalline (circle symbol) samples. The anomaly around 504 K corresponds to the melting temperature of elemental Sn in agreement with SEM analyses. The second anomaly at 800 K might be related to the structural transition. Note that we have extrapolated the temperature dependence of the specific heat linearly from 300 up to 820 K to calculate κ.

κ values (below 0.5 W m^{-1} K^{-1} above 500 K) are reached that presumably originate from strong intrinsic anharmonicity as suggested previously.[11] What is more surprising, however, is the fact that lower values are achieved in single crystals. Thanks to the presence of grain boundaries acting as an additional source of phonon scattering, similar or even lower values may have been expected in polycrystalline samples. The difference comes from a combination of higher diffusivity and specific heat values (Figure 4(b)) measured in the polycrystals. Noteworthy, the values measured at 300 K in the perpendicular direction approach those obtained in single crystals in early investigations (1.9 W m^{-1} K^{-1}).[15]

The combination of these favorable transport properties results in *ZT* values that rapidly increase with increasing temperature to reach a maximum *ZT* of 0.5 at 820 K (Figure 5). The *ZT* appears nearly isotropic, a situation already encountered in *p*-type BiSbTe alloys.[2,3] This value is

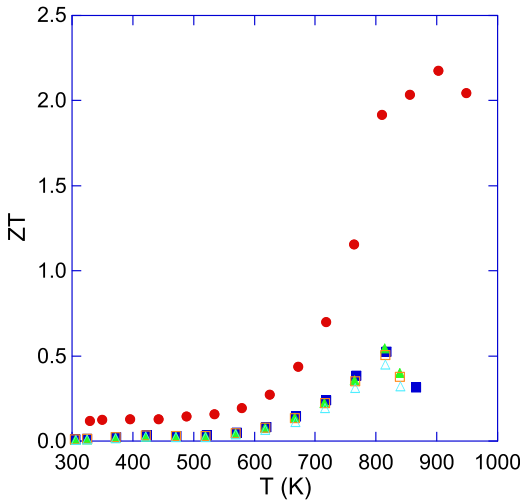

FIG. 5. Temperature dependence of the dimensionless figure of merit *ZT* of polycrystalline bulk samples of SnSe measured parallel and perpendicular to the pressing direction compared with the values obtained in single crystals.

significantly lower than those measured in single crystals by Zhao *et al.*[11] due to higher κ and ρ values. This is not to say that this phase does not deserve further attention. The values presented herein were obtained in non-optimized polycrystals, which leaves room for further improvement of the *ZT* values. In particular, SnSe is known to harbor deviations from stoichiometry as in the well-studied thermoelectric materials Bi_2Te_3 and PbTe.[2,3] Moreover, prior investigations on Te-substituted compounds indicate that *n*-type SnSe may be achieved.[14,16,17] Further studies should therefore tell us whether very high *ZT* values are achievable in this phase.

[1]H. J. Goldsmid, *Thermoelectric Refrigeration* (Temple Press Books, Ltd., London, 1964).
[2]*Thermoelectrics and Its Energy Harvesting*, edited by D. M. Rowe (CRC Press, 2012).
[3]*Thermoelectrics Handbook, Macro to Nano*, edited by D. M. Rowe (CRC Press, Taylor & Francis Group, Boca Raton FL, 2006).
[4]G. J. Snyder and E. S. Toberer, Nature Mater. **7**, 105 (2008).
[5]S. K. Bux, A. Zevalkink, O. Janka, D. Uhl, S. Kauzlarich, G. J. Snyder, and J.-P. Fleurial, J. Mater. Chem. A **2**, 215 (2014).
[6]A. Zevalkink, Y. Takagiwa, K. Kitahara, K. Kimura, and G. J. Snyder, Dalton Trans. **43**, 4720 (2014).
[7]T. Zhou, B. Lenoir, M. Colin, A. Dauscher, R. Al Rahal Al Orabi, P. Gougeon, M. Potel, and E. Guilmeau, Appl. Phys. Lett. **98**, 162106 (2011).
[8]P. Gougeon, P. Gall, R. Al Rahal Al Orabi, B. Fontaine, R. Gautier, M. Potel, T. Zhou, B. Lenoir, M. Colin, C. Candolfi, and A. Dauscher, Chem. Mater. **24**, 2899 (2012).
[9]X. Lu, D. T. Morelli, Y. Xia, F. Zhou, V. Ozolins, H. Chi, X. Zhou, and C. Uher, Adv. Energy Mater. **3**, 342 (2013).
[10]K. Suekuni, K. Tsuruta, T. Aiga, and M. Koyano, Appl. Phys. Express **5**, 051201 (2012).
[11]L.-D. Zhao, S.-H. Lo, Y. Zhang, H. Sun, G. Tan, C. Uher, C. Wolverton, V. P. Dravid, and M. G. Kanatzidis, Nature **508**, 373 (2014).
[12]C. Guillen, J. Montero, and J. Herrero, Phys. Status Solidi A **208**, 679 (2011).
[13]K. M. Chung, D. Wamwangi, M. Woda, M. Wuttig, and W. Bensch, J. Appl. Phys. **103**, 083523 (2008).
[14]S. Chen, K. Cai, and W. Zhao, Physica B **407**, 4154 (2012).
[15]J. D. Wasscher, W. Albers, and C. Haas, Solid State Electron. **6**, 261 (1963).
[16]H. Maier and D. R. Daniel, J. Electron. Mater. **6**, 693 (1977).
[17]W. Albers, C. Haas, H. Ober, G. R. Schodder, and J. D. Wasscher, J. Phys. Chem. Solids **23**, 215 (1962).